

Hemodynamic impacts of left coronary stenosis: A patient-specific analysis

THANAPONG CHAICHANA¹, ZHONGHUA SUN^{1*}, JAMES JEWKES²

¹ Discipline of Medical Imaging, Department of Imaging and Applied Physics, Curtin University, Perth, Western Australia, Australia.

² Fluid Dynamics Research Group, Department of Mechanical Engineering, Curtin University, Perth, Western Australia, Australia.

This study analyses the hemodynamic variations surrounding stenoses located at the left coronary bifurcation, and their influence on the wall shear stress (WSS) in realistic coronary geometries. Four patients with suspected coronary artery disease were chosen, and coronary models were reconstructed based on high-resolution CT data. The coronary stenoses were observed at the left circumflex and left anterior descending branches, resulting in a lumen narrowing of >50%. Flow analysis was performed using computational fluid dynamics, to simulate the cardiac flow conditions of the realistic individual patient geometry. Blood flow and WSS changes in the left coronary artery were calculated throughout the entire cardiac phases. Our results revealed that the recirculation regions were found at the post-stenotic locations. WSS was found to increase at the stenotic positions in all four patients. There is a strong correlation between coronary stenosis and the hemodynamic changes, which are reflected in blood flow pattern and WSS, based on the realistic left coronary geometries.

Key words: coronary artery disease, computational fluid dynamics, wall shear stress

1. Introduction

It is widely recognized that coronary artery disease is the primary cardiovascular disease, responsible for the development of major adverse cardiac events, leading to hemodynamic variations in the myocardium [1], [2]. Satisfactory results for the assessment of coronary plaques and coronary stenosis have been achieved with medical imaging techniques such as computed tomography (CT) and intravascular ultrasound [3], [4]. However, prediction of local stenosis progression in the specific patient with coronary artery disease remains intractable. The left coronary bifurcation is the anatomic location where plaque or stenosis tends to form, due to the angulation formed between the left anterior descending (LAD) and left circumflex (LCX) [5]-[7]. A recent study reported that wide angulations induce flow disturbances related to the stenotic progression [5]. Hemodynamic pa-

rameters such as wall shear stress (WSS) and flow velocity are the key factors that are used to describe the development of cardiovascular disease [1], [2], [5]. Previous studies have shown that low WSS resulted in endothelial cell dysfunction and the principal advancement of atherosclerosis [8], [9].

WSS and flow velocity provide additional information, which enables analysis of the progression of coronary stenosis [1], [5]. Early studies have shown that coronary lesions of >40% lumen stenosis caused the throttling of coronary blood flow speed, reducing volumetric blood flow [10]. The study of the influence of local stenoses upon blood flow changes in the left coronary artery is expected to improve our understanding of the pathogenesis of coronary disease. Thus, this research was conducted to investigate the impact of stenoses upon hemodynamic changes at the left coronary bifurcation, based on realistic geometry sampled from patients with suspected coronary artery disease.

* Corresponding author: Zhonghua Sun, Department of Imaging and Applied Physics, Curtin University, GPO Box, U1987, Perth, Western Australia 6845, Australia. Tel: +61 892667509, fax: +61 892662377, e-mail: z.sun@curtin.edu.au

Received: June 15th, 2012

Accepted for publication: June 25th, 2013

2. Materials and methods

2.1. Patient information

Four patients suspected of coronary artery disease in the left coronary main branches and bifurcations were included in this study. The CT volumetric data of each patient was rendered using medical imaging software Analyze 7.0 (Analyze Direct, Inc., Lexana, KS, USA) for generation of three-dimensional left coronary artery (LCA) geometries with inclusion of stenosis lesions. Each patient was found to have at least 50% lumen stenosis at the LAD and LCX on CT images. The demographics of sample patients are shown in Table 1. The medical imaging diagnosis of calcified plaques causing the lumen stenosis is displayed in Fig. 1. Imaging post-processing techniques were applied to create the LCA geometries with object-map reconstructions, semi-automatic modifying, post-process segmentation, with the details having been explained in previous studies [11], [12]. Three-dimensional LCA surfaces of four patients were remodeled, comprising of left main stem (LMS), LAD, LCX and its coronary trees. The surface geometries were saved in “STL format” for computational modeling. In summary, there were two patients with coronary stenosis in LCX branches and the other two patients had stenosis at LAD branches.

Table 1. Patient characteristics: patients with suspected coronary artery disease

No.	Age	Sex	Degree of bifurcation stenosis due to plaques		Bifurcation angle (°)
			Left anterior descending	Left circumflex	
A	50	Male	–	>50%	125
B	54	Female	–	>60%	95
C	56	Male	>50%	–	90
D	58	Female	>70%	–	85

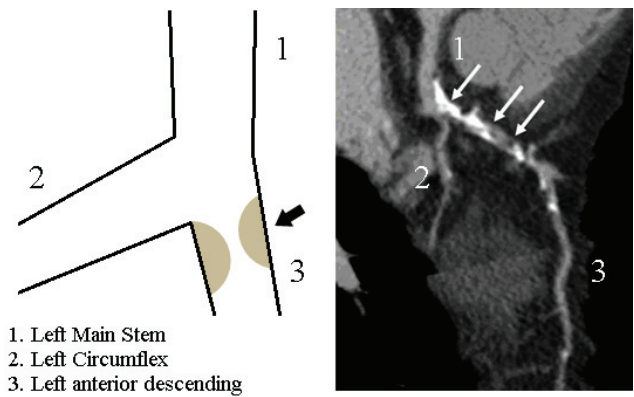


Fig. 1. Two-dimensional axial CT image identifies the calcified plaque positions (arrows in left image) and the diagram shows coronary stenosis located in the left anterior descending branch (arrows in right image)

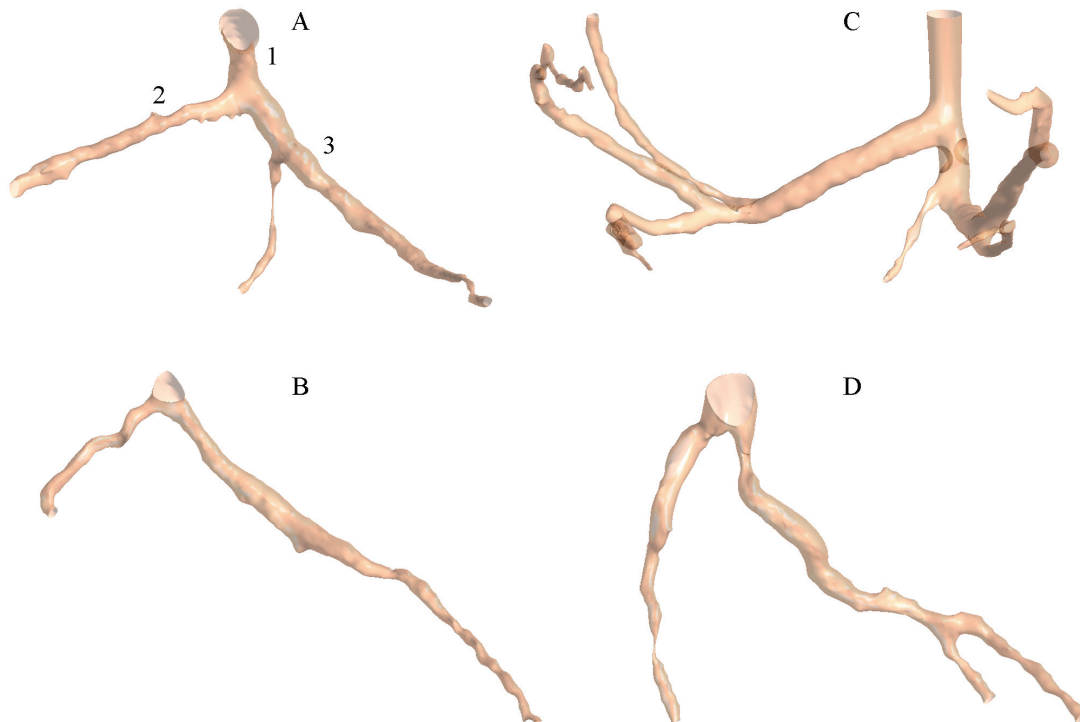


Fig. 2. The reconstructed left coronary artery geometries with diseased conditions in left main bifurcations with each model corresponding to the individual patient, as shown in Table 1

2.2. Computational modeling LCA with stenosis conditions

The reconstruction procedure used Blender version 2.48 (Blender Institute, Amsterdam, Netherlands) to modify the point clouds from each patient's STL data. Rough surfaces, and blood vessel tortuosity were retained to reflect true LCA disease conditions, however, unwanted data, soft tissues and motion-related artifacts were manually removed. The actual LCA geometries were analyzed in this research, as shown in Fig. 2. LCA geometries were saved in "STL format" for meshing procedure. The computational volume mesh was produced using ANSYS ICEM CFD version 12 (ANSYS, Inc., Canonsburg, PA, USA), our approach reflecting earlier studies [13], [14]. LCA mesh geometries were configured with hexahedral elements of around 9×10^5 cells. The computational mesh was saved in "GTM format" for solving.

2.3. Computational hemodynamic analysis

Transient computations were performed using physiologically-derived boundary conditions to reflect realistic *in vivo* conditions. The cardiac pulsatile velocity and pressures were reconstructed from pulsatile graphs taken from McDonald's Blood Flow in Arteries [15] using Matlab (MathWorks, Inc. Natick, MA,

USA). Velocity and pressures were applied at the main inlet (left main stem) and outlets (left anterior descending and left circumflex), respectively, for all of the LCA geometries [16]. Rheological properties were applied, with a blood density of 1060 kg/m^3 , blood viscosity of 0.0035 Pa s [17], [18]. Stenoses conditions were modeled as a rigid body [1], [5]. A no slip boundary condition was applied at the coronary walls, and blood viscosity was assumed to be Newtonian. The flow was assumed to be laminar and incompressible [19]. ANSYS CFX version 12 (ANSYS, Inc., Canonsburg, PA, USA) was used to solve the Navier–Stokes equations, requiring approximately 100 iterations per time-step within 1.0 second of pulsatile flow and pressure (1 time-step representing 0.0125 seconds). A converged solution was obtained for a residual target of less than 0.1×10^{-3} , and the computational time consumption was roughly 2 hours for each case. Wall shear-stress and hemodynamic profiles were calculated and visualized using ANSYS CFD-Post version 12 (ANSYS, Inc.).

3. Results

3.1. Impact of coronary stenosis upon hemodynamic variations at LCA

The analysis was performed based on realistic, *in vivo* physiological conditions during cardiac phases.

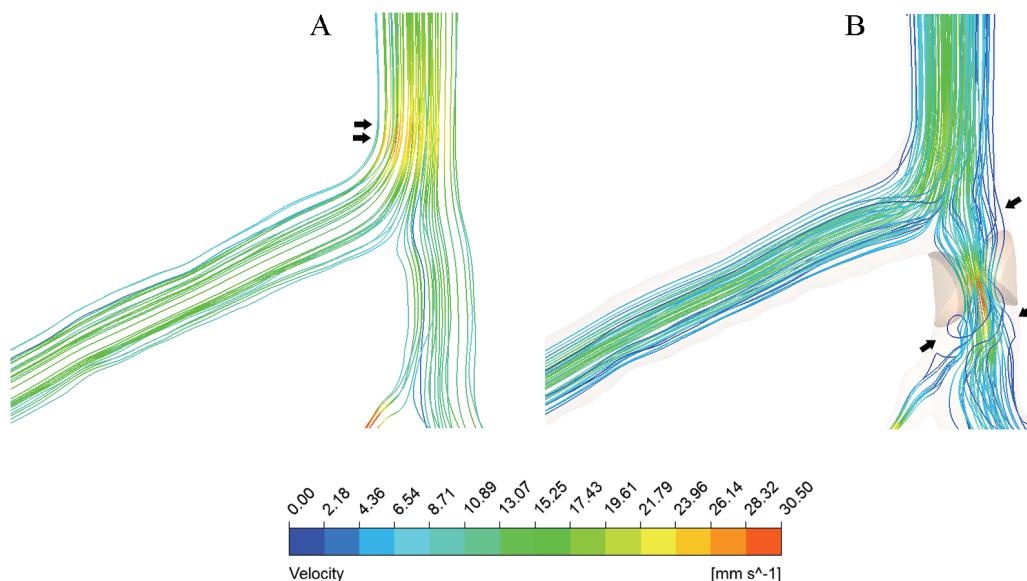


Fig. 3. Visualization of flow velocity patterns in Patient 'C' with coronary stenosis (A) and without stenosis (B) throughout the systolic peak of 0.4 s. Arrows indicate the areas of low flow velocity which occurred at pre- and post-stenosis locations. Double arrows in A show the regions of high flow velocity

The peak systolic and inner diastolic phases have been presented at the time of 0.2 sec and 0.7 sec, respectively. The simulation results displayed the effect of coronary stenosis located in the LAD and LCX branches on blood flow variations. The plaque's influence on hemodynamic changes at the left main coronary bifurcation is shown in Fig. 3. The velocity values ranged from 0 to 30.5 mm s^{-1} which were displayed in ten colored levels. The LCA geometry with diseased branches demonstrated a substantial flow velocity increase at the stenotic locations, which ranged from 28.32 to 30.50 mm s^{-1} (peak systolic) and 23.96 to 28.32 mm s^{-1} (middle diastolic, not shown). Maximum velocity was reached at LAD and LCX branches, where coronary stenosis caused significant coronary lumen narrowing. Locations of recirculation were found at post-stenosis positions in the LAD and LCX (Fig. 3).

3.2. Impact of coronary stenosis on WSS variations at LCA

WSS variations were calculated and visualized at the systolic and diastolic periods. The contour of ten colored levels was used to reveal the WSS values,

which ranged from 0 Pa to 3.50 Pa, as shown in Fig. 4. WSS distributions in the four study patients were similar, with high WSS found ranging from 3.25 Pa to 3.50 Pa at the locations where coronary stenosis caused lumen narrowing (Fig. 4). Low WSS values were found to range from 0 Pa to 0.25 Pa at the left coronary arteries (Fig. 4).

4. Discussion

This study demonstrates that coronary stenosis can substantially affect blood flow in the realistic left coronary artery geometries, causing variations of velocity and WSS. Results of this study assist our clinical understanding of the influence of coronary stenosis upon blood flow in coronary artery disease, which could lead to atherosclerotic progression.

Coronary stenoses are generally found at bifurcated locations, and main coronary branches such as LAD and LCX. Previous studies have reported that atherosclerotic plaques form at these coronary bifurcations [7], [16]. Current medical imaging techniques are excellent in demonstrating anatomical details [3], [20], [21], but are limited to providing the information

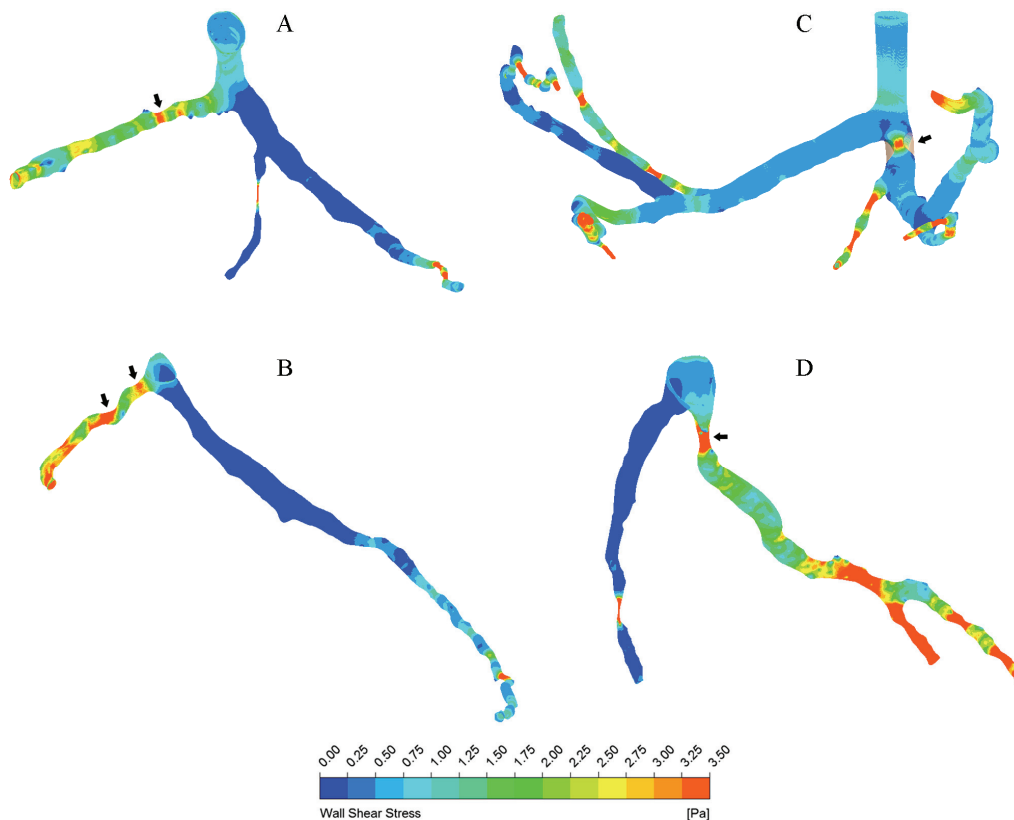


Fig. 4. Visualization of the WSS of four patients with coronary stenosis through the systolic peak of 0.4 s. Arrows indicate the distribution of high WSS which occurred at stenosis regions

on the alterations of hemodynamic parameters in coronary artery. Computational fluid dynamic analysis of remodeled coronary artery geometries enables the observation of hemodynamic changes, thus, offering additional information when compared to the diagnostic information acquired with modern imaging modalities [13], [14], [16].

There are two main factors, WSS and flow velocity that are commonly used to analyze hemodynamic changes, and quantify the influence of coronary stenosis on hemodynamic variations of human coronary artery. In this study, high WSS areas (arrows revealed in Fig. 4) were found in areas of coronary stenosis. This finding can be used to predict potential plaque rupture at the high WSS sites [2], [22]. Furthermore, low WSS regions (Fig. 4) were found in left coronary geometries, thus this may induce atherosclerotic development [7], [16]. Hemodynamic changes were found to increase at stenotic regions, and recirculation was also indicated at post-stenosis locations (arrows identified these changes in left image, as shown in Fig. 3). According to the flow analysis, the atherosclerotic plaques tend to form at post-stenotic positions, in low flow velocity, recirculating areas [7], [16]. This research provides an understanding of the influence of bifurcation stenosis at LAD and LCX branches on the WSS and flow velocity, and reveals the subsequent flow changes near to stenotic positions.

Current research studies have demonstrated that low WSS distributions were associated with atherosclerotic progression, and high WSS was regarded as a contributor to plaque rupture and thrombosis in atherosclerosis [2]. It has been shown that the atherosclerotic plaques located in the coronary main bifurcation may cause WSS and hemodynamic changes to their coronary trees [1], [5]. Some representative studies have revealed clinical information concerning the risk factor of atherosclerosis in coronary artery disease related to the bifurcation stenosis [23], [24]. Our results are consistent with these reports as we observed high WSS at stenotic locations and recirculating locations were found at post-stenotic positions.

Hemodynamic analysis of individual patients with realistic LCA geometries has some limitations that should be addressed. The stenosis models were assumed to be smooth, this assumption has been shown to be reasonable in previous studies [1], [5]. The coronary walls were considered rigid, and again this assumption is reasonable in this case [19]. In addition, the blood viscosity was assumed to be non-Newtonian, this can be significant in low flow conditions, however, in this configuration it has been shown

to be acceptable [19]. The sample size was small, as only four patients were included and this may not represent all types of coronary disease. Therefore, further studies will include a more representative range of diseased coronary geometries.

In conclusion, we analyzed the hemodynamic impact of coronary stenosis in realistic left coronary artery geometries with diseased regions between LAD and LCX branches. There is a direct influence of coronary stenosis in the left coronary artery upon the WSS and blood flow. The results of hemodynamic analysis indicate that coronary stenoses may increase the potential risk for the rupture and thrombosis of atherosclerotic plaques. Further analysis based on a larger number of patients with a wider range of types of coronary disease is required to validate our results.

References

- [1] CHAICHANA T., SUN Z., JEWKES J., *Impact of plaques in the left coronary artery on wall shear stress and pressure gradient in coronary side branches*, Computer Methods in Biomechanics and Biomedical Engineering, 2012, Epub ahead of print 1–11. DOI:10.1080/10255842.2012.671308
- [2] SAMADY H., ESHTEHARDI P., MCDANIEL, M.C., SUO J., DHAWAN S.S., MAYNARD C., TIMMINS L.H., QUYYUMI A.A., GIDDENS D.P., *Coronary artery wall shear stress is associated with progression and transformation of atherosclerotic plaque and arterial remodeling in patients with coronary artery disease*, Circulation, 2011, Vol. 124, 779–788.
- [3] SUN Z., DIMPUDUS F.J., NUGROHO J., ADIPRANOTO J.D., *CT virtual intravascular endoscopy assessment of coronary artery plaques: A preliminary study*, European Journal of Radiology, 2010, Vol. 75, e112–e119.
- [4] GIJSEN F.J., WENTZEL J.J., THURY A., LAMERS B., SCHURBIERS J.C., SERRUYS P.W., van der STEEN A.F., *A new imaging technique to study 3-D plaque and shear stress distribution in human coronary artery bifurcations in vivo*, Journal of Biomechanics, 2007, Vol. 40(11), 2349–2357.
- [5] CHAICHANA T., SUN Z., JEWKES J., *Computational fluid dynamics analysis of the effect of plaques in the left coronary artery*, Computational and Mathematical Methods in Medicine, 2012, Vol. 504367, 1–9.
- [6] ASAKURA T., KARINO T., *Flow patterns and spatial distribution of atherosclerotic lesions in human coronary arteries*, Circulation Research, 1990, Vol. 66, 1045–1066.
- [7] FUSTER V., LEWIS A., *Conner memorial lecture. Mechanisms leading to myocardial infarction: insights from studies of vascular biology*, Circulation, 1994, Vol. 90(4), 2126–2146.
- [8] NAM D., NI C., REZVAN A., SUO J., BUDZYN K., LLANOS A., HARRISON D., GIDDENS D., JO H., *Partial carotid ligation is a model of acutely induced disturbed flow, leading to rapid endothelial dysfunction and atherosclerosis*, American Journal of Physiology. Heart and Circulatory Physiology, 2009, Vol. 297(4), H1535–H1543.
- [9] ZARINS C.K., GIDDENS D.P., BHARADVAJ B.K., SOTTIURAI V.S., MABON R.F., GLAGOV S., *Carotid bifurcation atherosclerosis: quantitative correlation of plaque localization with*

- flow velocity profiles and wall shear stress*, *Circulation Research*, 1983, Vol. 53, 502–514.
- [10] GLAGOV S., WEISENBERG E., ZARINS C.K., STANKUNAVICIUS R., KOLETTIS G.J., *Compensatory enlargement of human atherosclerotic coronary arteries*, *The New England Journal of Medicine*, 1987, Vol. 316(22), 1372–1375.
- [11] SUN Z., WINDER R.J., KELLY B.E., ELLIS P.K., KENNEDY P.T., HIRST D.G., *Diagnostic value of CT virtual intravascular endoscopy in aortic stent-grafting*, *Journal of Endovascular Therapy*, 2004, Vol. 11(1), 13–25.
- [12] SUN Z., WINDER R.J., KELLY B.E., ELLIS P.K., HIRST D.G., *CT virtual intravascular endoscopy of abdominal aortic aneurysms treated with suprarenal endovascular stent grafting*, *Abdominal Imaging*, 2003, Vol. 28(4), 580–587.
- [13] SUN Z., CHAICHANA T., *Fenestrated stent graft repair of abdominal aortic aneurysm: hemodynamic analysis of the effect of fenestrated stents on the renal arteries*, *Korean Journal of Radiology*, 2010, Vol. 11(1), 95–106.
- [14] SUN Z., CHAICHANA T., *Investigation of the hemodynamic effect of stent wires on renal arteries in patients with abdominal aortic aneurysms treated with suprarenal stent-grafts*, *CardioVascular Radiology*, 2009, Vol. 32(4), 647–657.
- [15] NICHOLS W., O'ROURKE M., *McDonald's Blood Flow in Arteries*, Hodder Arnold, London, 2005, 326–327.
- [16] CHAICHANA T., SUN Z., JEWKES J., *Computation of haemodynamics in the left coronary artery with variable angulations*, *Journal of Biomechanics*, 2011, Vol. 44(10), 1869–1878.
- [17] BOUTSIANIS E., DAVE H., FRAUENFELDER T., POULIKAKOS D., WILDERMUTH S., TURINA M., VENTIKOS Y., ZUND G., *Computational simulation of intracoronary flow based on real coronary geometry*, *European Journal of Cardio-Thoracic Surgery*, 2004, Vol. 26, 248–256.
- [18] MILNOR W., *Hemodynamics*, Williams & Wilkins, Baltimore, 1989.
- [19] JOHNSTON B.M., JOHNSTON P.R., CORNEY S., KILPATRICK D., *Non-Newtonian blood flow in human right coronary arteries: steady state simulations*, *Journal of Biomechanics*, 2004, Vol. 37, 709–720.
- [20] SUN Z., CAO Y., *Multislice CT angiography assessment of left coronary artery: Correlation between bifurcation angle and dimensions and development of coronary artery disease*, *European Journal of Radiology*, 2011, Vol. 79, e90–e95.
- [21] FEUCHTNER G.M., CURY R.C., JODOCY D., FRIEDRICH G.J., BLUMENTHAL R.S., BUDOFF M.J., NASIR K., *Differences in coronary plaques composition by noninvasive computed tomography in individuals with and without obstructive coronary artery disease*, *Atherosclerosis*, 2011, Vol. 215, 90–95.
- [22] SLAGER C.J., WENTZEL J.J., GIJSEN F.J.H., THURY A., van der WAL A.C., SCHAAR J.A., SERRUYS P.W., *The role of shear stress in the destabilization of vulnerable plaques and related therapeutic implications*, *Nature Clinical Practice Cardiovascular Medicine*, 2004, Vol. 2, 456–464.
- [23] CHERUVU P.K., FINN A.V., GARDNER C., CAPLAN J., GOLDSTEIN J., STONE G.W., VIRMANI R., MULLER J.E., *Frequency and distribution of thin-cap fibroatheroma and ruptured plaques in human coronary arteries: a pathologic study*, *Journal of the American College of Cardiology*, 2011, Vol. 50, 940–949.
- [24] DILETTI R., ONUMA, Y., FAROOQ V., GOMEZ-LARA J., BRUGALETTA S., VAN GEUNS R.J., REGAR E., DE BRUYNE B., DUDEK D., THUESEN L., CHEVALIER B., MCCLEAN D., WINDECKER S., WHITBOURN R., SMITS P., KOOLEN J., MEREDITH I., LI D., VELDHOFF S., RAPOZA R., GARCIA-GARCIA H.M., ORMISTON J.A., SERRUYS P.W., *6-month clinical outcomes following implantation of the bioresorbable everolimus-eluting vascular scaffold in vessels smaller or larger than 2.5 mm*, *Journal of the American College of Cardiology*, 2011, Vol. 58, 258–264.